Advanced Science Letters
Vol. 2, 1–9, 2009

Solar Signals in Southern Hemisphere African Climate Since 1901

Joachim Rathmann* and Jucundus Jacobeit

Institute of Geography, University of Augsburg, Augsburg 86135, Germany

The present study intends to contribute to the understanding of solar-climate relationships in the context of climate variability in southern hemisphere Africa since the beginning of the 20th century. The study is based on the monthly HadSLP2 data set; sea surface temperature data are taken from the HadISST1.1 dataset, and high-resolution precipitation and temperature data are provided by the Climatic Research Unit (CRU). These data have been updated and improved within the Potsdam Institute for Climate Impact Research (PIK). Solar signals in the Southern Hemisphere climate system are identified in successive steps by using different statistical methods. Initially, *s*-mode varimax-rotated PCAs have been used to reduce the number of variables. The resulting time coefficients have further been analysed by spectrum and wavelet analyses. Additionally, correlation and composite analyses have been performed, using total solar irradiance and sunspot number data. In general, tropospheric effects of variable solar activity are concentrated on particular regions: Significant solar signals can be revealed in South African air temperatures during the boreal summer; in precipitation of East Africa and northern Namibia/southern Angola during winter and spring. SSTs in the southern equatorial Atlantic and SLP of the subtropical anticyclones over the Atlantic and Indian oceans include further significant solar signals in the study domain.

1. INTRODUCTION

Climate variations in semiarid regions of Africa have a strong socioeconomic impact because of large populations and limited natural resources. Understanding of past climate variations has an outstanding importance for seasonal forecasts, future climate projections and the crop and water management. In this context solar-climate relationships are an essential factor of uncertainty even if direct solar influence on climate change might be relatively small compared to recent man-made impacts. The climate system may respond to solar variability arising from the 27-day solar rotation, the 11-year solar cycle, century-scale sunspot minima and maxima and variations on longer time scales. The kind and amount of climatic response depend on internal feedbacks within the climate system itself and therefore might be detected only by particular techniques. The present study intends to contribute to the understanding of solar-climate relationships in context of climate variability during the past 100 years in southern hemisphere Africa, a continent with large fractions of semiarid regions and therefore particularly sensitive to climate variations and driving forcing factors. Solar signals in this part of the Southern Hemisphere climate system will be identified in successive steps by using different statistical methods (see Section 4). At first, however, a short overview on the state of the art is required (next section).

2. STATE OF RESEARCH

There have been hundreds of studies during the last decades concerning climate response to the 11-year sunspot cycle, ranging from sea level changes of Lake Victoria, temperature or precipitation at various stations up to changes in the upper atmosphere; but a coherent signal at the Earth's surface has not yet been established statistically or physically.[1] In spite of research for many decades the influence of solar activity changes on the climate of the earth is still characterised by a "low level of scientific understanding."[2] This might be due to the fact that many solar-climate links can be proofed statistically, whereas a clear physical cause-effect relation is still open to discussion, especially concerning climatic effects of solar radiation changes on different time scales. A study of Usoskin et al.[3] leads to the conclusion that the solar-climate influence during the last decades might be more important than known up to now: a reconstruction of sunspot numbers since the year 850 AD leads to the conclusion that since 1940 there exists a maximum sunspot number with respect to the whole period of more than 1000 years. Usoskin et al.[4] have recently extended this reconstruction back to 5000 BC emphasising that the modern high level of solar activity is very unusual even during the last 7000 years.

The sun influences the climate of the earth by its whole radiation spectrum, the so called solar wind and its influence on cosmic rays. Resulting solar signals can yet be traced on a wide range of vertical extent, starting in the ionosphere, mesosphere

*Author to whom correspondence should be addressed.

and upper stratosphere, going down to the tropospheric circulation and to the near surface climate, including the oceans and the sea ice distribution.[5–9] The most highly variable parts of the sun's radiation spectrum can be found at short wavelengths, e.g., the ultraviolet (UV). Variations of the solar UV irradiance are much bigger than variations in visible light. Thus, influences on the ozone layer are to be expected.[8] Actually a variation of the UV irradiance of 4% within the 11-year solar cycle leads to temperature changes in the lower stratosphere of 0.5 K.

However, a clear signal of the 11-year sunspot cycle in the stratosphere appears only when the data are stratified according to the different phases of the Quasi-Biennial Oscillation[11–13].[a] Furthermore, it has been detected that even the strength of the QBO is influenced by the sunspot cycle: the amplitude of both the QBO easterly and westerly phase is weaker during the solar cycle maximum than during the minimum.[13, 14] During the solar maximum of the QBO easterly phase a strengthening of the Antarctic polar vortex (the so called positive "annular mode") occurs. A positive stratospheric temperature anomaly can be observed in the tropic-subtropical region which can be explained by an adiabatic warming due to descending air. This warming results from a weakening of the Brewer-Dobson circulation.[b] Solar minima during the QBO easterly phase favour the occurrence of intensive polar stratosphere warmings. Such events take also place in the QBO westerly phase, but now during the solar maximum.[10, 14, 15] This warming is coupled to descending air over the polar regions leading to adiabatic cooling with upward motion on the summerly Northern Hemisphere thus opposing the positive solar signal and strengthening the Brewer-Dobson circulation.[14]

The far-reaching importance of the stratosphere for the tropospheric circulation should be emphasised especially in the solar-climatic context.[8, 16] The polar regions are, beside the tropics, of particular importance for transferring stratospheric signals downward into the troposphere.[17] The Southern Hemisphere "Annular mode" clearly shows significant connections between stratospheric and tropospheric circulation patterns (e.g., Ref. [16]). Salby and Callaghan[15] point out that the dynamical structure of the stratosphere reaches down to the troposphere. Other studies emphasise the striking effect of stratospheric anomalies on the troposphere, propagating downward in the Northern Hemisphere within 60 days.[18, 19] In the Southern Hemispheric troposphere anomalies originating from the stratosphere can still be identified after up to 90 days. Recent Southern Hemisphere climatic changes are reflected in an enforced zonal circulation especially during the summer months, manifested in the so called "Southern Hemisphere Annular Mode" (SAM). Thompson and Solomon[19] give evidence that these circulation changes are consistent with the stratospheric ozone depletion. The stratospheric polar vortex propagates downward into the troposphere until the early summer months, leading to a stronger tropospheric westerly flow. But many details regarding the downward propagation are still unclear, and further aspects of solar-stratosphere-climate coupling cannot be discussed here.

Some indications exist for tropospheric circulation changes due to the 11-year sunspot cycle, from both model studies (e.g., Refs. [6, 8, 20, 21]) and observational studies (e.g., Refs. [5, 7, 13, 22–24]). As a major result we know that during the QBO westerly phase at the solar maximum a strengthening of the tropospheric Hadley circulation develops,[13, 14] on the other hand a weakening during the easterly phase. This means that tropospheric solar signals differ according to the QBO phase. The influence on the Hadley circulation may result from altitude changes of the tropical tropopause which, in turn, are related to lower stratospheric circulation changes. A study, using the NCAR Whole Atmosphere Community Climate Model 6 (WACCM), shows the atmospheric response to changes within the 11-year solar cycle from the lower thermosphere down to the surface thereby revealing that near-surface temperature response is less than signals observed in reanalysis datasets.[8] Jury et al.[25] addressed possible QBO-precipitation links in Southern Africa by means of correlation analyses. They found that upper tropospheric easterly winds above the Southern African east coast are strengthened during the QBO easterly phase. These winds lead to upper tropospheric convergence and descending air masses over much of the Southern African subcontinent, whereas the QBO westerly phase enforces precipitation in that region by an intensified upper tropospheric westerly circulation within the west–east directed circulation cell.

Solar influences on cloud formation are another topic being addressed on the one hand by microphysical analyses,[26, 27] on the other hand by statistical correlations between cloud cover and solar irradiance including cosmic ray variations; possible influences have led to very controversial discussions on that subject.[28–32] Reliable global cloud cover data are available not before 1983 thus including only two solar cycles and therefore providing a restricted basis for sound conclusions.

Some studies analyse tropospheric climate data without considering stratospheric processes in detail. Thresher[33] for example shows Southern Hemisphere solar-climate relationships based on correlation analyses for selected time series. In doing so, he is able to indicate a quasi 11-year cycle in the course of the subpolar westerly winds, coupled with a shifting of 5° in the branch of the Hadley cell with maximum windspeed. Ruzmaikin et al.[34] discuss associations of the Nile water level with solar activity. Stager et al.[24] identify relations between the sunspot number and lake level data of Lake Victoria and other east African lakes during the 20th century. They assume that the effect of solar irradiance changes on the precipitation in East Africa might be amplified by interactions with SSTs, ENSO and, in general, the atmospheric circulation. Camp and Tung[35] apply composite analyses to detect the influence of the solar cycle on surface temperatures during the last decades. They obtain a significant signal and conclude that a globally averaged warming of almost 0.2 K between sunspot minimum and maximum is much larger than previously reported.

Surface warming is not restricted to land areas: Reid[36] uses SSTs as a proxy for the global surface temperature, because they represent more than 70% of the earth's surface, exhibit a bigger spatial coherence and have a lower temporal variability than global land temperatures. Reid shows in particular a high correlation of SST means (globally and basin-wide) and 11-year running means of the sunspot number during the past 130 years. The solar signal can be estimated in the order of 0.1 °C corresponding to a solar radiation forcing of 0.1 W/m^2.[36, 37] Moron et al.,[38] however, could not detect any coherent SST signal on a decadal time scale. Against that, other studies found oscillations in the range of 11 years in the tropical Atlantic Ocean.[39, 40]

[a] QBO: oscillation of the equatorial zonal wind between easterlies and westerlies in the tropical stratosphere with a mean period of 28 to 29 months.[10]

[b] A circulation pattern that sets up between equator and pole.

A detailed study explores the response of the oceanic mixed layer to the 11-year sunspot cycle. A 0.1 K/Wm^{-2} signal of the solar influence can be derived.[41] A later study makes clear that quasi-decadal signals in the upper oceans may develop without direct solar forcing.[42] Thus, it is still open to discussion in how far changes of solar activity might be reflected in oceanic temperatures or different atmosphere-ocean feedback mechanisms might lead to quasi-decadal variations. In conclusion, there are particular ways for a solar signal transport from the upper atmosphere into the oceans becoming manifest in atmospheric circulation changes. However, it is not the purpose of this paper to investigate these mechanisms and other ones mentioned in this overview. The aim of the present paper is rather to analyse near-surface data for the 20th century in order to identify particular regions where solar variability might contribute significantly to recent climate change and variability.

3. DATA

The Global Mean Sea Level Pressure (GMSLP2.1) data set was developed in collaboration of the Hadley Centre, the Meteorological Office (UK), CSIRO (Australia) and NIWA (New Zealand). It is a monthly gridded data set covering the period 1871–1994 with a 5° latitude by 5° longitude resolution. A recent version HadSLP2 replaces the HadSLP1 data which followed the GMSLP data and covered the period from 1850 to 2004. The data set is based on marine observations taken from ICOADS (International Comprehensive Ocean-Atmosphere Data Set) and land (terrestrial and island) observations from 2228 stations around the globe. More than 600 of them have time series longer than 100 years. These observational data have been quality checked and afterwards interpolated to the regular grid. A detailed description of the HadSLP2 data is given in Allan and Ansell.[43]

Sea Surface Temperature data are taken from the HadISST1.1 data developed by the UK Met. Office. The data start in 1870 having a spatial resolution of 1° × 1°. The SST grid is based on observational data which have been interpolated by a two-stage reduced-space optimal interpolation procedure.[44]

Monthly precipitation and temperature data are taken from the 0.5° × 0.5° Climate Research Unit (Norwich) CRU05-dataset covering initially the 1901–1998 period. The data include the whole global land area except for Antarctica and are based on station data.[45,46] These data have been widely used in climate research, and in the meantime new versions have been developed.[47–49] The present paper is based on that version which has been updated and improved within the Potsdam Institute for Climate Impact Research (PIK).[47]

As an indicator of solar activity changes over the past century, reconstructed total solar irradiance (TSI) data based on a statistical model calibrated with space-based measurements of solar radiative output has been used.[50]

4. METHODS

Principal Component Analysis (PCA) is a useful method to reduce a large number of variables to a limited number of independent factors. PCA is widely used in climate research in order to identify major patterns of atmospheric circulation, to pick out centres of atmospheric (or oceanic) variation or, generally, to reduce dimensions of original data and to remove linear dependencies between basic variables. There are two frequently used versions of PCA for parameter fields (e.g., SLP, temperature or precipitation) with time-space resolution: a first one defines variables according to the number of spatial units (stations, grid points or grid boxes), takes temporal observations as the individual realizations (cases) of these variables and is usually referred to as '*s*-mode' (*s*: space). A second one, in contrast, defines variables according to the number of temporal observations, takes the spatial units as their realizations and is referred to as '*t*-mode' (*t*: time). In the present context *s*-mode analyses have been performed whose loadings can be represented by maps displaying spatial centres of variation for each PC. *s*-mode PCA applied to monthly SST, SLP, temperature and precipitation data have been performed with orthogonal Varimax rotation[51,52] since mapping the loadings of unrotated PCs generally does not provide physically interpretable patterns.[53] The extraction of the PCs is based on the correlation matrix of the original variables. For determining the number of PCs to be extracted, the PC loadings are standardized in two different ways: once for each PC over all variables and once for each variable over all PCs. For the extraction of a particular PC the two standardized loading values have to exceed 1 for at least one input variable[54] reflecting both the relevance of this PC for the corresponding input variable and its relative importance in comparison to the other PCs. For precipitation, the spatial centres of variation are defined by groups of grid boxes with loadings higher than 0.5 on a particular PC. As temperature, SLP and SST do not show such a high spatial and temporal variability like precipitation, the regionalization by means of *s*-mode PCA could be done easier with an increased threshold of 0.7. Furthermore, the number of regions for temperature, SLP and SST is lower than for precipitation. All resulting PC time coefficients have further been submitted to different time series analyses (see below).

To receive a first impression of possible solar-climate connections, it is useful to do simple correlation analyses between solar activity indices and climate data. For this study the total solar irradiance (TSI) reconstruction of Lean et al. has been used.[50] Each grid box of the above-mentioned data has been correlated with TSI leading to different correlation maps. Of course these results have to be interpreted very carefully since even if they are highly significant, they might be misleading with respect to physical mechanisms. Based on these simple associations, further analyses have to be done in order to get robust indications of solar signals in the climate system of southern hemispheric Africa. One step consists of particular composite analyses calculating differences between composites of temperature, precipitation, SLP and SST for months above and below the long-term mean sunspot number, respectively. In addition, the same calculations have been done for months above (below) the 90th (10th) and 75th (25th) percentiles in order to check whether some results might only be a matter of chance.

Time-series analyses based on the time coefficients of the above-mentioned *s*-mode Principal Components have been performed in terms of autocorrelation, spectral variance and wavelet analyses. The aim of this approach is to identify cyclic components within the data.

Autocorrelation ("serial correlation") links data of a time series with itself by inserting gradually increasing time lags. It is only useful to find strong repeating patterns in the data. Spectral analysis is able to determine periodicities more precisely. It allows

to distinguish between cyclic forcing mechanisms of the climate system and broad-band resonances. The spectrum of a time series distributes its variance onto different frequencies. Indicated periodic signals, however, can vary in both amplitude and frequency over long periods of time; hence Wavelet analyses are increasingly used.

The last decades have seen a strong increase of interest in wavelets. They have been widely used for signal compression and denoising on the one hand and as a tool for analyzing time series on the other hand. Many climatological studies include wavelet analyses, too. For example, Mélice and Servain[55] use this method in their study on SST variability in the tropical Atlantic. Jury[56] analyses ENSO signals in Africa based on wavelet analyses. Frick et al.[57] apply this method on solar data. Fligge et al.[58] make use of wavelets in their study on the solar cycle length. Souza Echer et al.[59] apply the wavelet transformation on annual rainfall series.

Wavelet analyses allow to show a time-series signal simultaneously in time and frequency, a considerable advantage for analyzing non-stationary time series compared to the above-mentioned spectral analysis. The wavelet transformation allows to identify the main periodicities in a time series and at the same time their temporal evolution. In the present paper, a complex Morlet wavelet has been used as a so called mother wavelet, because it is the most adequate one to detect continuously variations of periodicities in the data. The Morlet wavelet is a plane wave modulated Gaussian function.[60] The continuous wavelet transformation W of a signal $x(t)$ can be defined as (cp.: Ref. [61], p. 2393, Ref. [55], p. 462):

$$W_x(b,a) = \frac{1}{a^{1/2}} \int_{-\infty}^{\infty} x(t)\psi^*\left(\frac{t-b}{a}\right) dt$$

a: dilation parameter
b: translation parameter
ψ: wavelet

The continuous wavelet transformation is able to calculate, based on the parameters a and b, a theoretically infinite number of wavelet functions. The applied software for these calculations is based on original routines from Torrence and Compo.[60]

All wavelet analyses have been carried out for each month separately concerning SST, SLP, temperature and precipitation data. Only the most striking results with significant signals will be presented. The corresponding graphs (Figs. 5 to 9) reproduce the signal duration on the horizontal axis i and the period of the oscillations on the vertical axis. Higher values in the corresponding plots indicate maxima of the spectral power depending on the period.

5. RESULTS

Differences of temperature-composites for months with sunspot maxima and minima are generally low and reach 0.7 K in April. During austral winter there is a clear signal with higher values in South Africa for increased solar activity, especially beyond the higher-order percentiles (Fig. 1). This might be due to the influence of changes in the direct solar radiation on the high pressure system which establishes in winter above the South African highlands.

Differences of precipitation composites, calculated in the same way, show increased precipitation during months of strengthened solar activity in East Africa for the long-rains period (Fig. 2).

Differences of SST composites show only very small values in the lower latitudes (not shown). This might be explained by two opposite effects: Higher solar activity raises tropical SSTs, but due to an enhanced evaporation at the same time, energy is removed from the surface, leading to lower SSTs. Further relationships can also be shown by correlation analyses, for example between the solar irradiance and SST-data (with time coefficients for the latter from a s-mode PCA): there are highly significant values ($r = 0.7$) for particular centres of SST variation in the midlatitudes between 50 °S and 60 °S (not shown).

Further results are based on time series analyses. As a first step autocorrelation analyses are used to get some indications on decadal-scale cyclic variability of the data. For that purpose, all time coefficients resulting from s-mode PCAs of the SST, SLP, temperature and precipitation data have been analysed in this respect. A striking decadal-scale cycle is revealed within the tropical Atlantic SST data with a spatial centre at 5 °S/10 °W, although this cycle is only significant at the 90% confidence level. This can be seen in Figure 3, based on selected months. But whether this is an internal cycle within the climate system or a direct solar-induced one can not be determined yet. However,

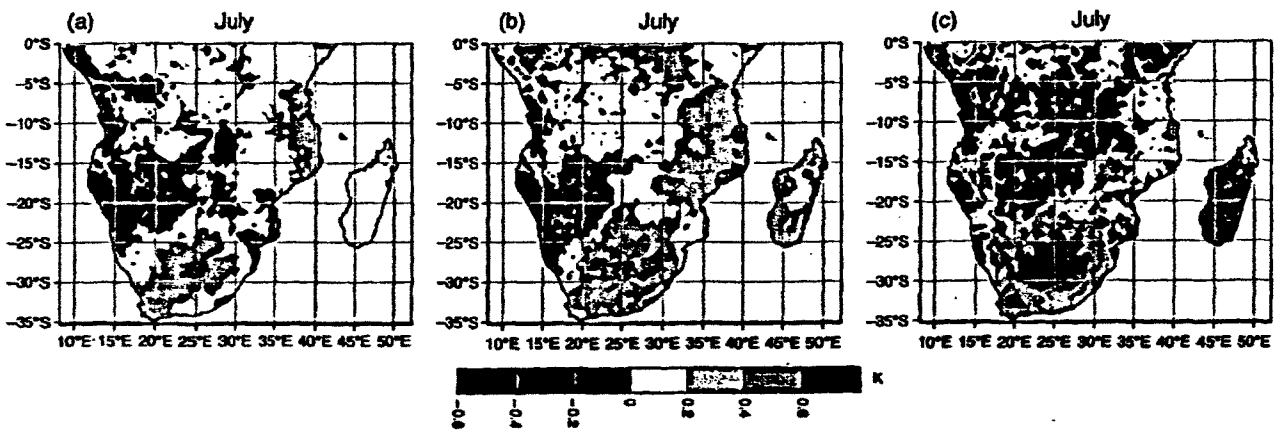

Fig. 1. (a) Differences of July temperature composites for sunspot numbers above and below the long-term mean (62.55 for 1901–2003), respectively; (b) for sunspot numbers above and below the 75th and 25th percentiles, respectively; (c) for sunspot numbers above and below the 90th and 10th percentiles, respectively.

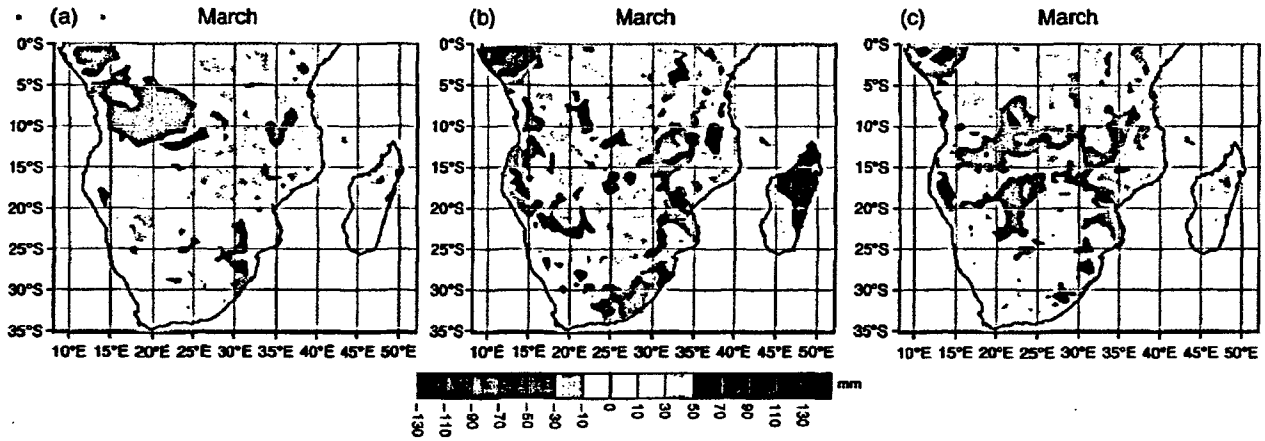

Fig. 2. (a) Differences of March precipitation composites for sunspot numbers above and below the long-term mean (62.55 for 1901–2003), respectively; (b) for sunspot numbers above and below the 75th and 25th percentiles, respectively; (c) for sunspot numbers above and below the 90th and 10th percentiles, respectively.

the results of SST-composite analyses (not shown) suggest lower SSTs during sunspot maxima, whereas simple correlation analyses would not support a solar influence.

The autocorrelation functions for monthly SST data (based on PC time coefficients) clearly indicate a periodicity on a quasi-decadal time scale. Similar results could be achieved for other climate variables and particular regions. Before summarizing these results, further examples from more sophisticated time series analyses will be discussed.

For instance, spectral analyses applied to the same time coefficients of SST-PCs as in Figure 3, representing the centres of SST variation in the southern equatorial Atlantic Ocean, confirm strong quasi-decadal signals with spectral maxima at 12.8 years for the months of May and August (Fig. 4). Although this is a little more than the mean solar cycle length, it might be a hidden solar signal, extended in frequency by passing the atmosphere. These striking maxima in the SST power spectra are significant at the 97.5% (May) and 99% (August) confidence levels, i.e., they are significantly different from white noise describing the spectral variance of randomly sampled data. A second maximum with a period of about 40 years reflects the long-term SST-trend.

The following figures show some selected examples of time-series with quasi-decadal signals resulting from wavelet analyses. The black lines outline the "cone of influence," i.e., the area that suffers from edge effects and therefore cannot really be interpreted. The wavelet spectra indicate that spectral maxima do not always extend over the whole period of time. This can be seen in Figure 5 for the wavelet transformation of the time coefficient of the February SST-PC in the southern equatorial Atlantic. A strong decadal signal is identified only since 1970 whereas this signal exists for the whole period during the other months (cf. January, Fig. 5). However, it may also be rather week during particular subperiods as in April and May between 1930 and 1960 (not shown), when the SST-trends were negative[62] which could indicate reduced solar influence. The high-frequency spectral maximum in February between 1940 and 1950 indicates a high amplitude during this decade which might be explained by data problems during the time of World War II.[44,63]

After all, results of wavelet analyses emphasise a quasi-decadal SST variability in the tropical Atlantic Ocean south of the equator, even with a shorter period than the 14-year signal found by Mélice and Servain[55] for a comparable region between 1964 and 1998.

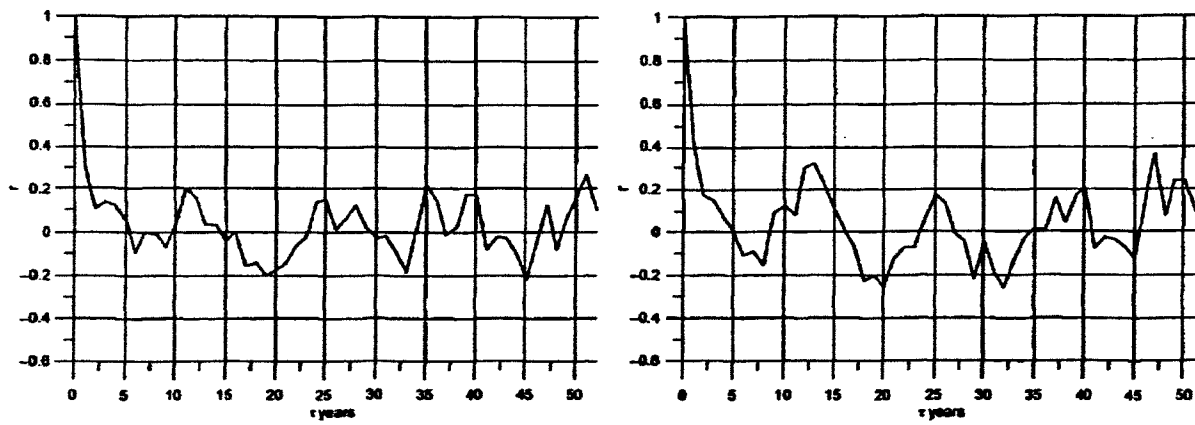

Fig. 3. Autocorrelation functions based on selected PC time coefficients of monthly SST data 1901–2003 for May (left) and August (right). All the selected s-mode PCs describe centres of SST variation in the southern equatorial Atlantic. The autocorrelation coefficients are scaled on the y-axis, the time steps on the x-axis.

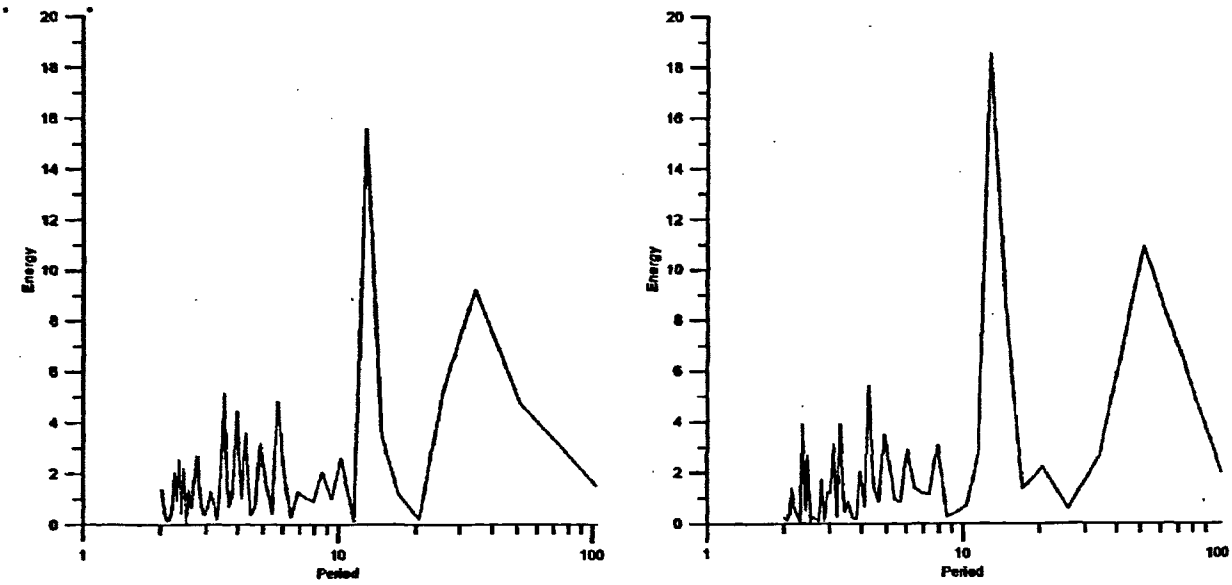

Fig. 4. Power spectra of the PC time coefficients 1901–2003 for SST centres of variation in the southern equatorial Atlantic for May (left) and August (right). Periods (in years) on a logarithmic al scale.

The analysis of SLP data shows only few spectral maxima on a decadal time scale. The most important case refers to the St. Helena high pressure system over the central South Atlantic Ocean during all seasons but most pronounced in southern winter, when the high pressure cells are intensified. For example during June (Fig. 6) a corresponding spectral maximum can be traced throughout the whole 20th century. However, it was considerably weaker between 1935 and 1950. Maybe the shift from a longer spell of predominantly lower intensity to a phase of higher central pressure during these years can account for this pattern.[64]

A spectral peak on a decadal time scale can also be identified in the wavelet power spectrum for the time coefficients of a temperature-PC representing the region of South Africa (see Fig. 7 for June). This possible solar signal is controlled by the anticyclone above the southern Atlantic Ocean which itself shows a spectral peak at the same period (Fig. 6). The wavelet power spectrum of Figure 7 shows also a small "island" of high-frequency power between 1960 and 1970 which is due to short-term fluctuations in the PC-time coefficients at that time (strong interannual variability). Such phenomena recur in several analyses but are not addressed in particular since the focus of this study lies on quasi-decadal signals.

Turning to investigations on possible solar signals in precipitation time series, initial correlation analyses with solar irradiance data revealed significant coefficients for Namibia and Angola. Just the same regions indicate a significant quasi-decadal variability which could be pointed out by means of autocorrelation and spectral analyses (not shown). Additional wavelet analyses, based on the monthly time coefficients of the *s*-mode precipitation-PCs representing this region, also show spectral maxima on this time scale (see Fig. 8 as an example). A comparable signal for East Africa (March) is considerably weaker but

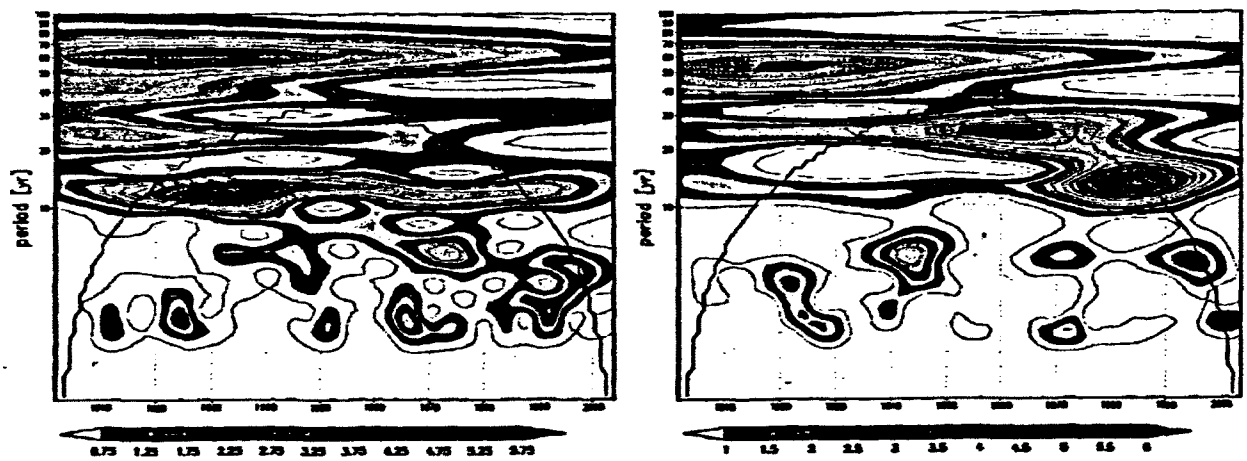

Fig. 5. Wavelet power spectra of the PC time coefficients 1901–2003 for SST centres of variation in the southern equatorial Atlantic for January (left) and February (right). The periods are shown on the *y*-axis with a logarithmic scale, the years 1901–2003 on the *x*-axis. The colour scale gives the wavelet power of a particular period during a definite section of time. Black lines outline the "cone of influence" (see text).

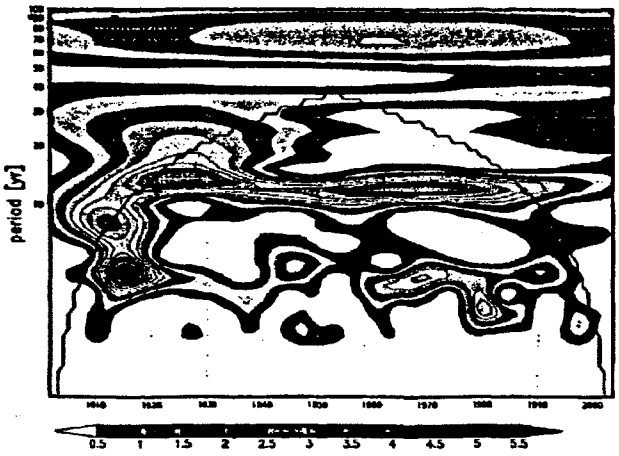

Fig. 6. As Figure 5 but for the PC time coefficient June 1901–2003 of the *s*-mode sea-level pressure PC representing the region of the Southern Atlantic subtropical anticyclone.

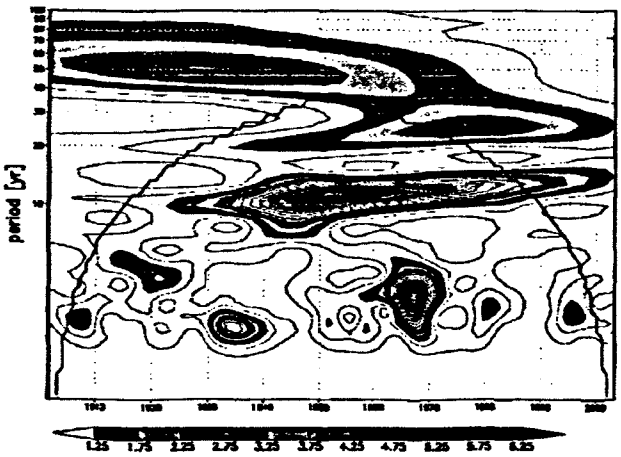

Fig. 7. As Figure 5 but for the PC time coefficient June 1901–2003 of the *s*-mode temperature PC representing the region of South Africa.

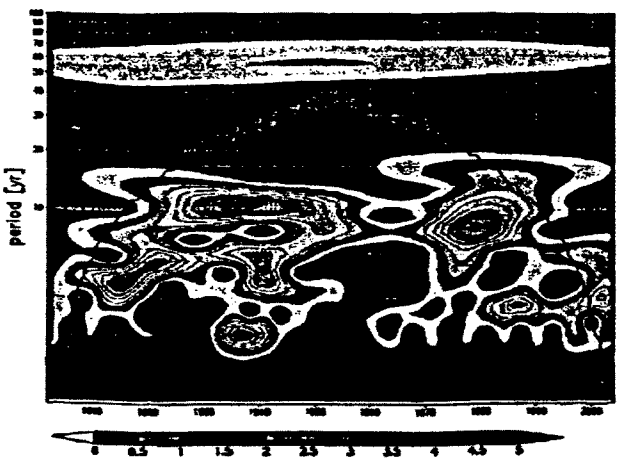

Fig. 8. As Figure 5 but for the PC time coefficient April 1901–2003 of the *s*-mode precipitation PC representing the region around Angola.

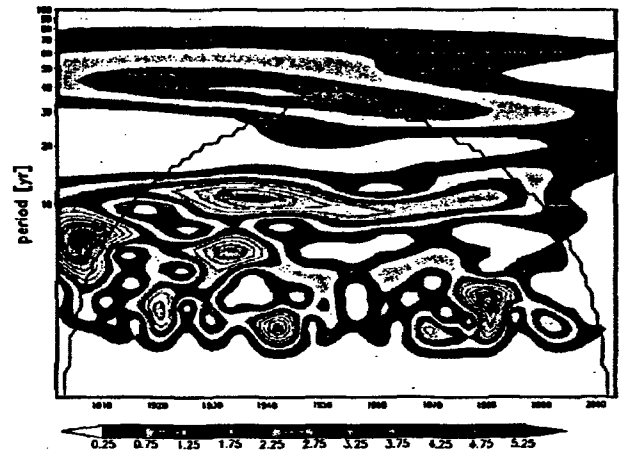

Fig. 9. As Figure 5 but for the PC time coefficient March 1901–2003 of the *s*-mode precipitation PC representing the region of East Africa.

very dominant during the first third of the 20th century (Fig. 9), when solar forcing was stronger compared to greenhouse gas forcing. The increased precipitation might be caused by solar impacts on the Indian Ocean Dipole[65] which strongly influences the East African precipitation, and by a stronger Hadley circulation during periods of higher solar activity.[66]

6. SUMMARY AND CONCLUSIONS

Variable solar activity influences the earth's climate on various time scales. A quantification of these influences including a sound derivation of signal transports through the atmosphere is still a challenging task. In the present paper some statistical relationships between solar activity and the climate of southern Africa on a quasi-decadal time scale have been identified since the beginning of the 20th century based mainly on different time series analyses (autocorrelation, spectral and wavelet analyses) in addition to simple correlation and composite analyses. However, such results are not unambiguous since peaks in power spectra might be due to different reasons including the big domain of internal variability within the climate system. Thus, a real physical causality can not be established by these analyses, it is only possible, in combination with correlation and composite analyses, to identify some indications on physical factors that might be driving forces of observed climate variability. As the solar forcing is of global dimension, one should expect a global-scale

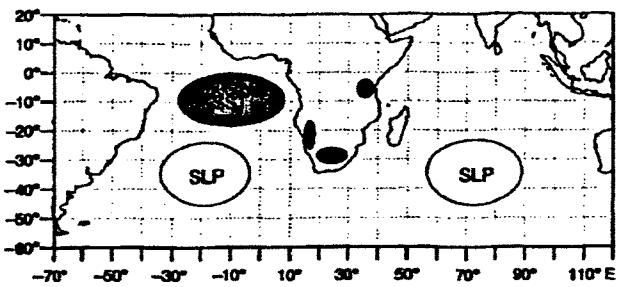

Fig. 10. Synopsis of regions for which solar signals in SST, SLP, Precipitation (*P*) or Temperature (*T*) data have been identified during the 1901–2003 period.

response. But it has be shown that solar signals concentrate on particular regions (see the following discussion). With respect to southern hemispheric Africa, some distinct solar signals have been found in various climatic data sets. Figure 10 summarises these results by specifying those regions with robust indications for a substantial solar influence.

Maximum significant correlations exist between solar irradiance and SST data in the middle to high southern latitudes. However, this seems to reflect rather the long-term trend of the SST data than a real solar signal according to results from composite and time-series analyses. The latter, however, indicate a distinct quasi-decadal signal in the equatorial Atlantic SST data. Since oceans can damp and delay atmospheric signals, the detected spectral maximum at 12.8 years might reflect the solar cycle. For clarifying whether this is a direct or an indirect solar influence, further analyses of upper atmospheric data have to be done in the future.

Other regions showing possibly solar-induced climate variability are located in the subtropical high pressure systems above the southern Atlantic and southern Indian Oceans. Stronger solar activity leads obviously to a light strengthening of these anticyclones. This relationship can be explained by a stronger direct solar influence and an intensified Hadley circulation, respectively.

A solar influence on southern hemispheric winter temperatures in South Africa is comparatively strong. Both composite and time-series analyses have shown robust relationships which might be explained by a direct radiation influence on the nearly cloud-free winterly high pressure system above central South Africa.

Precipitation in northern Namibia/southern Angola exhibits a striking quasi-decadal signal, and correlation analyses suggest a relationship with changing solar activity. Positive precipitation anomalies during the 'long rains' could be identified in East Africa during periods of increased solar activity. This might be explained by an intensified Hadley circulation during these periods. Stronger highs (see above) can contribute to a more vigorous circulation within the ITCZ which, in turn, can increase convective rainfall during the tropical rainy seasons. Furthermore, higher solar activity might raise tropical SSTs and lead to higher precipitation in East Africa by influences on the Indian Ocean Dipole pattern.[65] On the other hand, it has been revealed that precipitation in southern Africa is meanwhile reduced (Fig. 2). This pattern is remarkably similar to an El-Niño-induced precipitation pattern. However, this contrasts with a mechanism including a favoured occurrence of La Niñas during phases of enhanced solar forcing.[67,68] Increased solar activity leads to higher evaporation over the nearly cloud-free regions in the subtropics, and this might also lead to lower SSTs. Stronger regional Hadley and Walker cells due to the increased atmospheric moisture content mean a stronger upward vertical motion in tropical latitudes and a corresponding intensified subsidence in the subtropical regions leading to a reduction of the cloud cover and therefore to an increasing solar irradiance input.[66] These surface feedbacks might explain how a small solar signal is amplified in local climate, and the solar impact on African precipitation might thus be explained by El Niño "as a mediator of the solar influence on climate."[67]

Another mechanism to explain solar induced precipitation changes might be reduced galactic cosmic rays during times of higher solar activity which could lead to a reduced cloud cover because of a decreasing number of cloud condensation nuclei.[24,28] This again could increase direct insolation on the earth's surface leading to enhanced convection and precipitation.

Quasi-decadal signals as those identified in this study might be generated by solar forcing or by natural internal mechanisms which–in turn—might be caused by an indirect solar signal transport through the atmosphere. Due to lacking knowledge of physical signal transport mechanisms and to limited upper atmospheric data, it is far beyond this study to give an ultimate conclusion on the physical reality of solar-climate relationships. Further studies should trace in detail signal transports within the atmospheric circulation from the upper source region down to the near-surface climate, and precise cause-effect-chains should be analysed within a detailed vertical profile. Finally, it should be determined in how far recently increasing trends in solar activity which superimpose the 11-year solar cycle, enforce or modify the solar fingerprints in the Southern Hemisphere climate system.

References and Notes

1. R. E. Benestad, Solar Activity and Earth's Climate, Springer, London (2002).
2. IPCC, Climate Change 2007. Contribution of Working Group I to the Fourth Assessment Report of the IPCC. The Physical Science Basis, Cambridge University Press, Cambridge (2007), p. 203.
3. I. G. Usoskin, S. K. Solanki, M. Schüssler, K. Mursula, and K. Alanko, *Phys. Rev. Lett.* 91, 211101-1 (2003).
4. I. G. Usoskin, S. K. Solanki, and M. Korte, *Geophys. Res. Lett.* 33, L08103 (2006).
5. H. Gleisner and P. Thejll, *Geophys. Res. Lett.* 30, 1711 (2003).
6. J. D. Haigh, *Phil. Trans. R. Soc. Lond. A* 361, 95 (2003).
7. H. van Loon, G. A. Meehl, and J. M. Arblaster, *J. of Atmospheric and Sol.-Terr. Phys.* 66, 1767 (2004).
8. D. R. Marsh, R. R. Garcia, D. E. Kinnison, B. A. Boville, F. Sassi, S. C. Solomon, and K. Matthes, *J. Geophys. Res.* 112, D23306 (2007).
9. A. Ruzmaikin, *Adv. in Space Res.* 40, 1146 (2007).
10. M. P. Baldwin, L. J. Gray, T. J. Dunkerton, K. Hamilton, P. H. Haynes, W. J. Randel, J. R. Holton, M. J. Alexander, I. Hirota, T. Horinouchi, D. B. A. Jones, J. S. Kinnersley, C. Marquardt, K. Sato, and M. Takahashi, *Rev. Geophys.* 39, 179 (2001).
11. H. van Loon and K. Labitzke, *Space Sciences Rev.* 94, 259 (2000).
12. K. Labitzke, *Meteorol. Zeitschrift* 10, 83 (2001).
13. K. Labitzke, *J. of Atmospheric and Sol.-Terr. Phys.* 67, 45 (2005).
14. K. Labitzke, *Meteorol. Zeitschrift* 12, 209 (2003).
15. M. L. Salby and P. Callaghan, *J. Climate* 17, 34 (2004).
16. D. W. J. Thompson, M. P. Baldwin, and S. Solomon, *J. Atmospheric Sciences* 16, 708 (2005).
17. A. Stohl, H. Wernli, P. James, M. Bourqui, C. Forster, M. A. Liniger, P. Seibert, and M. Sprenger, *Bull. Americ. Met. Soc.* 84, 1565 (2003).
18. M. P. Baldwin and T. J. Dunkerton, *J. of Atmospheric and Sol.-Terr. Phys.* 67, 71 (2005).
19. D. W. J. Thompson and S. Solomon, *Science* 296, 895 (2002).
20. K. Matthes, Dissertation, Fachbereich Geowissenschaften, FU Berlin (2003), p. 227.
21. K. Matthes, Y. Kuroda, K. Kodera, and U. Langematz, *J. Geophys. Res.* 111, D06108 (2006).
22. K. Coughlin and K. K. Tung, *J. Geophys. Res.* 109, d21105 (2004).
23. M. Lockwood and C. Fröhlich, *Proceed. Roy. Soc. A* 463, 2447 (2007).
24. J. C. Stager, A. Ruzmaikin, D. Conway, P. Verburg, and P. J. Mason, *J. Geophys. Res.* 112, D15106 (2007).
25. M. R. Jury, C. Mc Queen, and K. Levey, *Theor. Appl. Climatol.* 50, 103 (1994).
26. B. A. Tinsley, *Space Science Rev.* 94, 231 (2000).
27. B. A. Tinsley, G. B. Burns, and L. Zhou, *Adv. in Space Res.* 40, 1126 (2007).
28. H. Svensmark, *Space Science Rev.* 93, 155 (2000).
29. N. Marsh and H. Svensmark, *Space Science Rev.* 107, 317 (2003).
30. J. E. Kristjánsson, A. Staple, J. Kristiansen, and E. Kaas, *Geophys. Res. Lett.* 29, 2107 (2002).
31. J. E. Kristjánsson, J. Kristiansen, and E. Kaas, *Adv. in Space Res.* 34, 407 (2004).
32. P. Laut, *J. Atmospheric and Sol.-Terr. Phys.* 65, 801 (2003).
33. R. E. Thresher, *Int. J. Climatol.* 22, 901 (2002).
34. A. Ruzmaikin, J. Feynman, and Y. L. Yung, *J. Geophys. Res.* 111, D21114 (2006).
35. C. D. Camp and K. K. Tung, *Geophys. Res. Lett.* 34, L14703 (2007).
36. G. C. Reid, *J. Geophys. Res.* 96, 2835 (1991).

37.* G. C. Reid, *Space Science Rev.* 94, 1 (2000).
38. V. Moron, R. Vautard, and M. Ghil, *Clim. Dyn.* 14, 545 (1998).
39. M. E. Mann and J. Park, *J. Geophys. Res.* 99, 25819 (1994).
40. V. M. Mehta and T. Delworth, *J. Climate* 8, 172 (1995).
41. W. B. White, J. Lean, D. R. Cayan, and M. D. Dettinger, *J. Geophys. Res.* 102, 3255 (1997).
42. W. B. White, M. D. Dettinger, and D. R. Cayan, *J. Geophys. Res.* 180, 3248 (2003).
43. R. Allan and T. Ansell, *J. Climate* 19, 5816 (2006).
44. N. A. Rayner, D. E. Parker, E. B. Horton, C. K. Folland, L. V. Alexander, D. P. Rowell, E. C. Kent, and A. Kaplan, *J. Geophys. Res.* 108, 4407 (2003).
45. M. New, M. Hulme, and P. Jones, *J. Climate* 12, 829 (1999).
46. M. New, M. Hulme, and P. Jones, *J. Climate* 13, 2217 (2000).
47. H. Österle, F.-W. Gerstengarbe, and P. C. Werner, *Terra Nostra* 6, 326 (2003).
48. T. D. Mitchell, T. R. Carter, P. D. Jones, M. Hulme, and M. New, Tyndall Centre Working Paper 55. Tyndall Centre for Climate Change Research (2004).
49. T. D. Mitchell and P. D. Jones, *Int. J. Climatol.* 25, 693 (2005).
50. J. Lean, J. Beer, and R. Bradley, *Geophys. Res. Lett.* 22, 3195 (1995).
51. R. W. Preisendorfer, Principal Component Analysis in Meteorology and Oceanography, Elsevier, New York (1988).
52. H. von Storch and F. W. Zwiers, Statistical Analysis in Climate Research, Cambridge University Press, Cambridge (1999).
53. R. Huth, *Meteorol. Atmos. Phys.* 59, 217 (1996).
54. J. Jacobeit, *Die Erde* 124, 63 (1993).
55. J.-L. Mélice and J. Servain, *Clim. Dyn.* 20, 447 (2003).
56. M. R. Jury, *African J. of Marine Science* 28, 41 (2006).
57. P. Frick, D. Galyagin, D. V. Hoyt, E. Nesme-Ribes, K. H. Schatten, D. Sokoloff, and V. Zakharov, *Astronomy and Astrophysics* 328, 670 (1997).
58. M. Fligge, S. K. Solanki, and J. Beer, *Astronomy and Astrophysics* 346, 313 (1999).
59. M. P. Souza Echer, E. Echer, D. J. Nordemann, N. R. Rigozo, and A. Prestes, *Clim. Change* 87, 489 (2008).
60. C. Torrence and G. P. Compo, *Bull. Americ. Met. Soc.* 79, 61 (1998).
61. K.-M. Lau and H. Weng, *Bull. Americ. Met. Soc.* 76, 2391 (1995).
62. J. Rathmann, Klima- und Zirkulationsvariabilität im südhemisphärischen Afrika seit Beginn des 20. Jahrhunderts, *Uni. Augsburg* (2008) (submitted).
63. N. A. Rayner, P. Brohan, D. E. Parker, C. K. Folland, J. J. Kennedy, M. Vanicek, T. Ansell, and S. F. B. Tett, *J. Climate* 19, 446 (2006).
64. H. Mächel, A. Kapala, and H. Flohn, *Int. J. Climatol.* 18, 1 (1998).
65. J. T. Nugroho, *Bull. Astr. Soc. India* 35, 575 (2007).
66. G. A. Meehl, W. M. Washington, T. M. L. Wigley, J. M. Arblaster, and A. Dai, *J. Climate* 16, 426 (2003).
67. J. Emile-Geay, M. Cane, R. Seager, A. Kaplan, and P. Almasi, *Paleoceanography* 22, PA3210 (2007).
68. M. E. Mann, M. A. Cane, S. E. Zebiak, and A. Clement, *J. Climate* 18, 447 (2005).

Received: 10 July 2008. Accepted: 11 September 2008.